Twelve-Lead ECG Reconstruction from Single-Lead Signals Using Generative Adversarial Networks

Jinho Joo[1], Gihun Joo[1], Yeji Kim[2], Moo-Nyun Jin[2], Junbeom Park[2(✉)], and Hyeonseung Im[1(✉)]

[1] Kangwon National University, Chuncheon 24341, Republic of Korea
{wnwlsgh111,joo9327,hsim}@kangwon.ac.kr
[2] Ewha Womans University Medical Center, Seoul 07985, Republic of Korea
{mnjin31,parkjb}@ewha.ac.kr

Abstract. Recent advances in wearable healthcare devices such as smartwatches allow us to monitor and manage our health condition more actively, for example, by measuring our electrocardiogram (ECG) and predicting cardiovascular diseases (CVDs) such as atrial fibrillation in real-time. Nevertheless, most smart devices can only measure single-lead signals, such as Lead I, while multichannel ECGs, such as twelve-lead signals, are necessary to identify more intricate CVDs such as left and right bundle branch blocks. In this paper, to address this problem, we propose a novel generative adversarial network (GAN) that can faithfully reconstruct 12-lead ECG signals from single-lead signals, which consists of two generators and one 1D U-Net discriminator. Experimental results show that it outperforms other representative generative models. Moreover, we also validate our method's ability to effectively reconstruct CVD-related characteristics by evaluating reconstructed ECGs with a highly accurate 12-lead ECG-based prediction model and three cardiologists.

Keywords: ECG reconstruction · Biosignal synthesis · Generative model

1 Introduction

Although these days smart healthcare devices such as smartwatches can be used to monitor a single-lead electrocardiogram (ECG) for Lead I and detect cardiovascular diseases (CVDs) such as atrial fibrillation (AF), multichannel ECGs such as twelve-lead signals are still required to diagnose more complex CVDs such as left and right bundle branch blocks (LBBBs and RBBBs) or myocardial

J. Joo and G. Joo—Contributed equally as first authors.

Supplementary Information The online version contains supplementary material available at https://doi.org/10.1007/978-3-031-43990-2_18.

H. Greenspan et al. (Eds.): MICCAI 2023, LNCS 14226, pp. 184–194, 2023.
https://doi.org/10.1007/978-3-031-43990-2_18

infarction. To proactively deal with such intricate CVDs, therefore, one may need to undergo a 12-lead ECG measurement at a hospital and utilize 12-lead ECG-based deep learning algorithms for predicting CVDs [3,4,15,18], which can be a cumbersome process in everyday life. It is neither plausible to train a prediction model using only single-lead ECGs measured by smart devices as it is not possible to correctly label complex CVDs for them in the first place. To address this problem, in this paper, we propose a novel generative adversarial network (GAN) [13], called EKGAN, that can faithfully reconstruct 12-lead ECGs only from single-lead ones.

Although the ECG synthesis problem is not new, most previous studies have focused on utilizing it for data augmentation purpose as it is difficult to collect a sufficient amount of labeled ECGs (with CVDs) for developing prediction models. For example, many researchers have focused on synthesizing realistic ECGs using variants of autoencoders and GANs [5,6,9–11,14,22,23]. These methods can be useful for training prediction models, but it is unclear how they can be leveraged with commonly available wearable devices that can measure only single-lead ECGs. Meanwhile, another line of work has focused on reconstructing the corresponding (missing) ECGs from only a few actual lead signals [2,7,17,21], usually generating 12 leads from three leads including Lead I and II. We note here that if we know Lead I and II, then all six limb leads can be derived by Willem Einthoven's law [8] and Goldberger's law [12]. Thus, their reconstruction problem indeed reduces to the problem of reconstructing six precordial leads.

Our work differs significantly from previous studies, as we generate all 11 remaining leads simultaneously from only a single lead. Thus, our method can be used to bridge commonly available wearable devices that can measure only Lead I and high-performance deep learning-based prediction models using 12-lead ECGs. To the best of our knowledge, our work is the first to reconstruct all 12 leads simultaneously from a real single lead. By using the approach in [6], one can also generate all 12 leads, but only incrementally. Our proposed method EKGAN employs two generators and one 1D U-Net [19] discriminator to capture CVD-specific characteristics and correlation patterns between Lead I and the remaining leads from ECG training data. Experimental results show that the reconstruction performance of EKGAN outperforms other representative generative models such as Pix2Pix [16], CycleGAN [24] and CardioGAN [20] under various metrics. We also evaluated the practical applicability of our method by applying an existing 12-lead ECG-based CVD prediction model [18] to the reconstructed ECGs. To this end, we consider AF, LBBB, and RBBB, among which LBBB and RBBB require multichannel ECGs to detect. Moreover, three cardiologists examined reconstructed ECGs to see if they accurately reflected the important CVD-related characteristics of the original ECGs. All the results confirm the effectiveness and usefulness of our method, thus enabling preventive healthcare with smart wearable devices for CVDs. For reproducibility, the source code of EKGAN is available at https://github.com/knu-plml/ecg-recon.

2 Methods

In this section, we introduce a novel conditional GAN for ECG reconstruction, called EKGAN, which is based on Pix2Pix [16] but employs an additional label generator G_L and uses a 1D U-Net discriminator instead of a PatchGAN discriminator. Its overall structure is shown in Fig. 1. The inference generator G_I takes a Lead I signal and generates corresponding 12-lead signals, while the label generator G_L takes the same input as G_I and simply returns the same signal. The whole purpose of G_L is to enable G_I's encoder to learn the important characteristics of Lead I. To this end, the latent vector produced by G_I's encoder is approximated to that of G_L's encoder so that G_I's decoder can produce more detailed ECGs that are closely correlated with the input Lead I signals. The discriminator D distinguishes 12-lead ECGs generated by G_I and the original ECGs. The whole process is repeated, adversarially learning G_I and D.

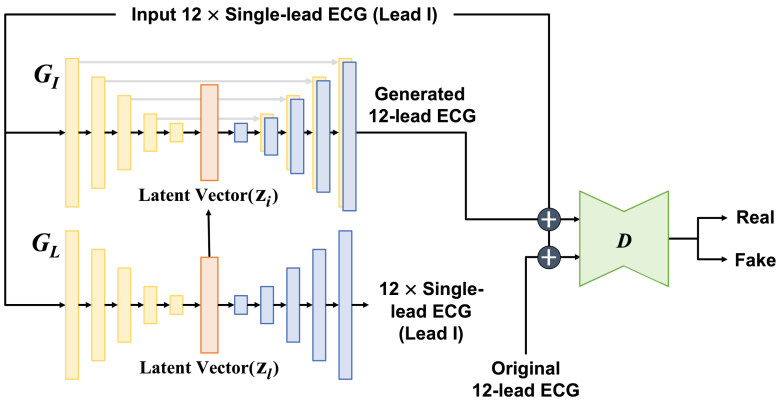

Fig. 1. Overall structure of EKGAN. G_I, inference generator; G_L, label generator; D, discriminator.

2.1 Generator

Inference Generator. The inference generator G_I is based on Pix2Pix's 2D U-Net generator and consists of an encoder and a decoder (Fig. 1). It takes an input of size $(16, 512, 1)$: 16 for 12 replicated signals of the input single lead plus 4 zero padding, 512 for the length of the ECG signal, and 1 for the channel size. More specifically, to generate 12-lead signals from single-lead signals, an input single-lead signal of length 512 is copied 12 times and two rows of zeros are added to both the top and bottom. Each original 12-lead ECG is arranged in the order of Lead I, II, III, aVR, aVL, aVF, and V1–V6, and is also zero padded. The encoder consists of five blocks each of which consists of convolution, batch normalization, and Leaky ReLU layers (an exception is the first block which excludes batch normalization). The numbers of convolution filters are

$64, 128, 256, 512, 1024$, while the kernel size is set to $(2, 4)$. The stride size is $(2, 2)$ except for the last block whose stride size is $(1, 2)$. The decoder is the inverse of the encoder and takes the encoder output as input. It also consists of five blocks each of which consists of concatenation, deconvolution, batch normalization, and ReLU layers (exceptions are the first block, which excludes concatenation, and the last block, which only uses concatenation and deconvolution). The numbers of deconvolution filters are $512, 256, 128, 64, 1$, while the kernel size is set to $(2, 4)$. The stride size is $(2, 2)$ except for the first block whose stride size is $(1, 2)$. From the second block, the output of the previous decoder block and that of the corresponding encoder block are concatenated and used as input.

Label Generator. An autoencoder-based model like U-Net [19] should create a latent vector in the encoder that represents the features of input data well. Then, the decoder should be learned to generate a target-like output from the latent vector. When training a U-Net, however, as we only use the reconstruction loss between the original and generated data, we cannot accurately determine how well the latent vector captures the essential features of the input (because there is no ground truth for the latent vector). In this paper, as a workaround, we use a label generator G_L which takes Lead I signals and returns the same signals. Accordingly, the latent vector produced by G_L's encoder would represent the features of the input accurately and thus can be used as ground truth for G_I's encoder. By doing so, G_I's decoder can produce a 12-lead ECG that is not only realistic but also closely associated with the input Lead I signal. The structure of G_L is similar to that of G_I, but it does not incorporate concatenation between the encoder and decoder. We experimentally validate the effectiveness of the label generator in Sect. 3.

2.2 Discriminator

In 12-lead ECGs, each lead has its own characteristics and thus it is important for a discriminator to analyze each lead signal individually at the pixel level. If a standard 2D convolution-based discriminator is used, as for image-to-image translation, which uses 2D patches, then the unique characteristics of each lead signal may be intermixed with others, which may in turn degrade the reconstruction quality. To prevent this problem, instead, we use a 1D U-Net discriminator D, which has the same layer architecture as G_L. D takes as input either G_I's output or an original 12-lead ECG, which is concatenated with G_I's input. In the encoder, the numbers of convolution filters are $32, 64, 128, 256, 512$, kernel sizes are $64, 32, 16, 8, 4$, and stride sizes are $4, 4, 4, 2, 2$. The decoder has the inverse structure of the encoder as in the two generators, except that it uses a sigmoid activation function at the last layer.

2.3 Loss

The objective of EKGAN is similar to that of other conditional GANs except that it uses the label generator G_L to train the inference generator G_I. Let us

write e_i for 12 replicated ECG segments from the input single-lead ECG for G_I and e_o for the corresponding ground-truth 12-lead ECG segments. In addition, let z_i and z_l be the latent vectors produced by the encoders of G_I and G_L, respectively. We use the following adversarial loss and L1 losses:

$$\begin{aligned}
\mathcal{L}_{\text{adv}}(G_I, D) &= \mathbb{E}_{e_i,e_o}[\log D(e_i, e_o)] + \mathbb{E}_{e_i}[\log(1 - D(e_i, G_I(e_i)))] \\
\mathcal{L}_{\text{L1}}(G_I) &= \mathbb{E}_{e_i,e_o}[||e_o - G_I(e_i)||_1] \\
\mathcal{L}_{\text{L1}}(G_L) &= \mathbb{E}_{e_i}[||e_i - G_L(e_i)||_1] \\
\mathcal{L}_{\text{LV}}(G_I, G_L) &= \mathbb{E}_{z_i,z_l}[||z_i - z_l||_1]
\end{aligned}$$

where the last one is the latent vector loss for the inference generator.

Then, the objective of EKGAN is defined as:

$$G_I^* = \arg \min_{G_I,G_L} \max_D \{\mathcal{L}_{\text{adv}}(G_I, D) + \lambda \mathcal{L}_{\text{L1}}(G_I) + \alpha \mathcal{L}_{\text{LV}}(G_I, G_L)\}$$

where λ and α control the relative importance of each function. Note that $\mathcal{L}_{L1}(G_L)$ is used solely for training G_L and thus not included in the objective equation. Through a grid search, we determined $\lambda = 50$ and $\alpha = 1$, and these values have been used in the following experiments unless otherwise stated.

3 Evaluation

This section introduces our dataset and its preprocessing. Then, we extensively evaluate EKGAN in terms of its reconstruction performance. We also assess its applicability using an existing prediction model with proven performance [18] and with three cardiologists.

3.1 Experimental Setup

Datasets. To develop and evaluate EKGAN, we used about 326,000 ECGs collected from Ewha Womans University Mokdong and Seoul Hospitals between May 23, 2017, and November 30, 2022. Specifically, we first selected ECGs with LBBB, RBBB, and AF from the dataset and randomly selected normal sinus rhythm (NSR) ECGs in a 1:1 ratio to reduce the bias of the generative models. For the label information, we simply used the interpretation result of the ECG machine. Next, for a test set for CVD multi-label classification and cardiologists' examination, we randomly chose 100 ECGs for each disease and 300 NSR ECGs. Then, the remaining dataset was randomly divided into train and validation sets in an 8:2 ratio. Table 1 shows the configuration of the final dataset. We note here that since AF and NSR may coexist with LBBB and RBBB, the number of classes is different from the total number of data. The generative models were trained using the train set and evaluated using the validation set. The CVD prediction model was trained using the train and validation sets where the latter was used for hyperparameter tuning. Finally, 12-lead ECGs were generated by using both the validation and test sets, and their quality was evaluated by

using the predictive model, *i.e.,* by comparing the classification performance with the original 12-lead ECGs and the generated ones, and examined by three cardiologists.

Table 1. Summary of the dataset. LBBB, Left Bundle Branch Block; RBBB, Right Bundle Branch Block; AF, Atrial Fibrillation; NSR, Normal Sinus Rhythm.

	LBBB	RBBB	AF	NSR	Total Classes	Total Data
Train	1,635	9,537	20,287	29,746	61,205	59,492
Validation	421	2,409	5,075	7,437	15,342	14,874
Test	102	108	140	460	810	600

Data Preparation. The 12-lead ECG data used in this study were measured for 10 s and the sampling rate is 500 Hz. To reduce the measurement noise, for each ECG signal, we remove the first 1 s and use only approximately the next 8.2 s (length of 4,096), while excluding the remaining part. In addition, for each 12-lead ECG, we normalize each lead signal individually, because if the amplitudes of 12-lead signals are significantly different from each other, the ones with small amplitudes may be ignored when predicting CVD. More specifically, for each signal, we first apply min-max normalization to $[-1, 1]$ and then a band-pass filter with lower and upper cutoff frequencies $[0.05, 150]$ as some fine details and important characteristics disappear when using a high lower cutoff frequency or a low upper cutoff frequency [1]. Finally, we downsample 4,096 lengths to 512 lengths.

Training and Test. All experiments were conducted on a workstation with an NVIDIA RTX 8000 and using TensorFlow 2.8. For comparisons, we implemented not only EKGAN but also Pix2Pix [16], CycleGAN [24], and CardioGAN [20] with minor modifications so that they can be applied to ECG data. In particular, for unpaired training of CycleGAN and CardioGAN, the input and label data were separated and shuffled independently. Moreover, due to the cycle consistency loss, Lead I of the label data was replaced with zero padding. All models were trained for 10 epochs, with the learning rate of 1e-4 until 5 epochs after which weight decay of 0.95 was applied per epoch. The kernel-initializer was sampled from a normal distribution $\mathcal{N}(0, 0.02^2)$.

3.2 Reconstruction Performance

Table 2 shows the reconstruction performance of EKGAN and other methods for the validation data in terms of root mean square error (RMSE), mean absolute error (MAE), percentage root mean square difference (PRD), maximum mean discrepancy (MMD), and mean absolute error for heart rates (MAE_{HR}). For all metrics, EKGAN significantly outperforms other methods, confirming the

effectiveness of its label generator and 1D U-Net discriminator for pixel-level learning of ECG signals. Meanwhile, CycleGAN and CardioGAN, which are based on unpaired training, are not suitable for 12-lead ECG reconstruction. Figure 2 shows examples of reconstructed 12-lead ECGs by various methods from the Lead I, where EKGAN produces the most faithful reconstruction of the original ECG.

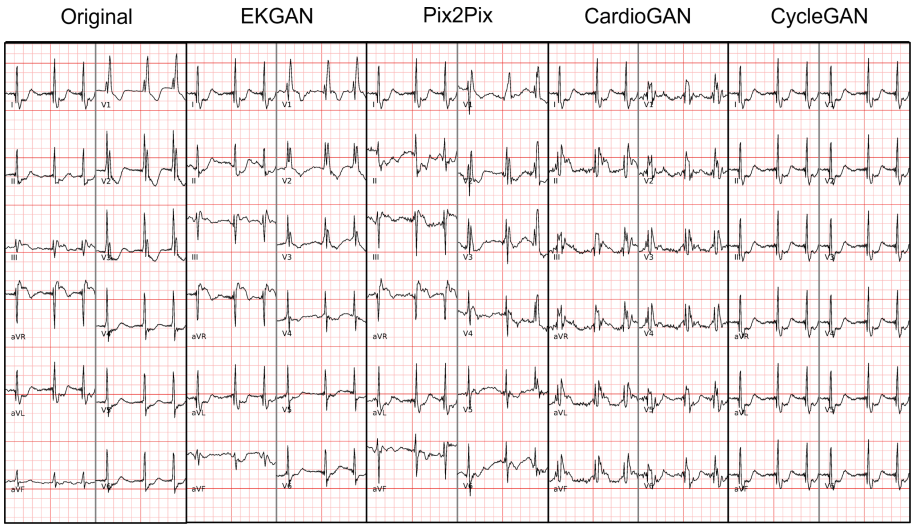

Fig. 2. Qualitative comparisons of various methods. The first column shows a sample original 12-lead ECG with RBBB and AF, while the rest was reconstructed from the original Lead I signal.

Table 2. Reconstruction performance of each method for the validation data.

Method	RMSE	MAE	PRD	MMD	MAE_{HR}
Pix2Pix	0.38	0.30	8.43	0.07×10^{-3}	27.68
CycleGAN	0.62	0.49	13.18	0.46×10^{-3}	24.16
CardioGAN	0.52	0.43	11.32	0.21×10^{-3}	24.09
EKGAN (proposed)	**0.32**	**0.25**	**6.95**	$\mathbf{0.04 \times 10^{-3}}$	**20.51**

Table 3. Performance of different variants of EKGAN for the validation data.

Method	RMSE	MAE	PRD	MMD	MAE_{HR}
Pix2Pix	0.38	0.30	8.43	0.07×10^{-3}	27.68
EKGAN w/o 1D discriminator	0.37	0.29	8.13	0.06×10^{-3}	24.06
EKGAN w/o label generator	0.35	0.28	7.73	0.05×10^{-3}	25.83
EKGAN (proposed)	**0.32**	**0.25**	**6.95**	$\mathbf{0.04 \times 10^{-3}}$	**20.51**

Table 3 shows the performance of different variants of EKGAN, that is, showing the effectiveness of our 1D discriminator and label generator. 'EKGAN w/o 1D discriminator' uses Pix2Pix's PatchGAN discriminator instead of our 1D U-Net discriminator. 'EKGAN w/o label generator' excludes a label generator and uses only an inference generator. We observe that the use of 1D discriminator is more effective than the use of a label generator, but using both results in a greater improvement over Pix2Pix for reconstructing 12-lead ECG signals.

Table 4. CVD multi-label classification results for the test data (F1-score). All results were obtained by using the algorithm proposed in [18].

Dataset	LBBB	RBBB	AF
Results reported in [18]	1.00	0.94	0.87
Original ECGs	0.92	0.97	0.92
Reconstructed ECGs by Pix2Pix	0.81	0.92	0.82
Reconstructed ECGs by EKGAN	0.94	0.96	0.88

Table 5. Concordance rate of three cardiologists for the test and reconstructed ECGs.

	LBBB	RBBB	AF	NSR
Cardiologist 1	96.32	92.31	93.65	93.65
Cardiologist 2	91.53	91.69	92.54	92.54
Cardiologist 3	94.77	92.24	91.06	91.06
Average	94.21	92.08	92.42	92.42

3.3 Reconstruction Quality Evaluation

To evaluate the applicability and quality of ECG signals reconstructed by EKGAN, we use a highly accurate prediction model for CVDs [18]. The model can predict six diseases by analyzing a 12-lead ECG, among which we choose LBBB, RBBB, and AF. We choose LBBB and RBBB as they require analysis of multi-lead ECGs and AF as it can be already predicted using commonly available wearable devices. This allows us to indirectly check if EKGAN is able to generate diverse ECG signals capturing different characteristics for each disease. Table 4 shows the multi-label classification results for the test set. Since the dataset used in [18] differs from ours, the performances using their datasets and ours are also slightly different, but both seem to perform well. We observe that the F1-scores when using the dataset reconstructed by EKGAN are comparable to those when using the original dataset and consistently better than those when using the ones reconstructed by Pix2Pix.

Table 5 shows the concordance rate between the test ECGs and the corresponding reconstructed ones by EKGAN, evaluated by three cardiologists. We

randomly shuffled the original and reconstructed ECGs, and each cardiologist reviewed every ECG if it exhibited LBBB, RBBB, AF, or NSR. Then, for each case, the concordance rate is calculated as the ratio of pairs of original and corresponding reconstructed ECGs such that a cardiologist's read result coincides among all data pairs. We note here that since each ECG must exclusively include either AF or NSR, their concordance rates are the same. The results confirm that the reconstructed ECGs by EKGAN effectively capture the important characteristics of the original ones.

4 Conclusion

This paper studies a novel problem of reconstructing 12-lead ECGs from single-lead ECGs. To address this problem, we propose a novel conditional GAN, called EKGAN, based on Pix2Pix, which consists of two generators and one 1D U-Net discriminator. Experimental results show that EKGAN significantly outperforms other representative generative models such as Pix2Pix, CycleGAN, and CardioGAN, and is able to reconstruct 12-lead ECGs that faithfully capture the essential characteristics of the original 12-lead ECGs useful for predicting CVDs. Therefore, we expect that numerous deep learning models based on 12-lead ECGs with proven performance could be applied to smart healthcare devices that can measure only single-lead signals. It would be also interesting to investigate if our method is applicable to more complex CVDs such as acute myocardial infarction, which require a more detailed analysis of 12-lead ECGs by cardiologists.

Acknowledgments. This research was supported by "Regional Innovation Strategy (RIS)" through the National Research Foundation of Korea (NRF) funded by the Ministry of Education (MOE) (2022RIS-005). This work was also supported by the NRF grant funded by the Korea government (MSIT) (No. RS-2023-00208094 and RS-2023-00242528) and by Institute of Information & communications Technology Planning & Evaluation (IITP) grant funded by the Korea government (MSIT) (No. RS-2022-00155966, Artificial Intelligence Convergence Innovation Human Resources Development (Ewha Womans University)).

References

1. Philips DXL ECG Algorithm Physician's Guide. 2nd Edn. Publication number 453564106411 (2009)
2. Atoui, H., Fayn, J., Rubel, P.: A novel neural-network model for deriving standard 12-lead ECGs from serial three-lead ECGs: application to self-care. IEEE Trans. Inf. Technol. Biomed. **14**(3), 883–890 (2010)
3. Attia, Z.I., et al.: An artificial intelligence-enabled ECG algorithm for the identification of patients with atrial fibrillation during sinus rhythm: a retrospective analysis of outcome prediction. The Lancet **394**(10201), 861–867 (2019)
4. Bos, J.M., Attia, Z.I., Albert, D.E., Noseworthy, P.A., Friedman, P.A., Ackerman, M.J.: Use of artificial intelligence and deep neural networks in evaluation of patients with electrocardiographically concealed long QT syndrome from the surface 12-lead electrocardiogram. JAMA Cardiol. **6**(5), 532–538 (2021)

5. Chen, J., Liao, K., Wei, K., Ying, H., Chen, D.Z., Wu, J.: ME-GAN: learning panoptic electrocardio representations for multi-view ECG synthesis conditioned on heart diseases. In: Chaudhuri, K., Jegelka, S., Song, L., Szepesvari, C., Niu, G., Sabato, S. (eds.) Proceedings of the 39th International Conference on Machine Learning. Proceedings of Machine Learning Research, vol. 162, pp. 3360–3370. PMLR, 17–23 July 2022
6. Chen, J., Zheng, X., Yu, H., Chen, D.Z., Wu, J.: Electrocardio panorama: synthesizing new ECG views with self-supervision. In: Zhou, Z.H. (ed.) Proceedings of the Thirtieth International Joint Conference on Artificial Intelligence, IJCAI-21, pp. 3597–3605 (8 2021)
7. Cho, Y., et al.: Artificial intelligence algorithm for detecting myocardial infarction using six-lead electrocardiography. Sci. Rep. **10**, 20495 (2020)
8. Einthoven, W.: The different forms of the human electrocardiogram and their signification. The Lancet. **179**(4622), 853–861 (1912)
9. Golany, T., Lavee, G., Tejman Yarden, S., Radinsky, K.: Improving ECG classification using generative adversarial networks. Proc. AAAI Conf. Artif. Intell. **34**(08), 13280–13285 (2020)
10. Golany, T., Radinsky, K.: PGANs: personalized generative adversarial networks for ECG synthesis to improve patient-specific deep ECG classification. Proc. AAAI Conf. Artif. Intell. **33**(01), 557–564 (2019)
11. Golany, T., Radinsky, K., Freedman, D.: SimGANs: simulator-based generative adversarial networks for ECG synthesis to improve deep ECG classification. In: III, H.D., Singh, A. (eds.) Proceedings of the 37th International Conference on Machine Learning. Proceedings of Machine Learning Research, vol. 119, pp. 3597–3606. PMLR, 13–18 July 2020. https://proceedings.mlr.press/v119/golany20a.html
12. Goldberger, A.L., Goldberger, Z.D., Shvilkin, A.: Chapter 4 - ECG Leads. In: Goldberger, A.L., Goldberger, Z.D., Shvilkin, A. (eds.) Goldberger's Clinical Electrocardiography (Ninth Edition), pp. 21–31, 9th Edn. Elsevier (2018)
13. Goodfellow, I., et al.: Generative adversarial nets. In: Ghahramani, Z., Welling, M., Cortes, C., Lawrence, N., Weinberger, K. (eds.) Advances in Neural Information Processing Systems, vol. 27. Curran Associates, Inc. (2014)
14. Hossain, K.F., Kamran, S.A., Tavakkoli, A., Pan, L., Ma, X., Rajasegarar, S., Karmaker, C.: ECG-Adv-GAN: detecting ECG adversarial examples with conditional generative adversarial networks. In: 2021 20th IEEE International Conference on Machine Learning and Applications (ICMLA), pp. 50–56 (2021)
15. Hughes, J.W., et al.: Performance of a convolutional neural network and explainability technique for 12-lead electrocardiogram interpretation. JAMA Cardiol. **6**(11), 1285–1295 (2021)
16. Isola, P., Zhu, J.Y., Zhou, T., Efros, A.A.: Image-to-image translation with conditional adversarial networks. In: 2017 IEEE Conference on Computer Vision and Pattern Recognition (CVPR), pp. 5967–5976 (2017). https://doi.org/10.1109/CVPR.2017.632
17. Lee, J., Kim, M., Kim, J.: Reconstruction of precordial lead electrocardiogram from limb leads using the state-space model. IEEE J. Biomed. Health Inform. **20**(3), 818–828 (2016)
18. Ribeiro, A.H., et al.: Automatic diagnosis of the 12-lead ECG using a deep neural network. Nat. Commun. **11**, 1760 (2020)
19. Ronneberger, O., Fischer, P., Brox, T.: U-Net: convolutional networks for biomedical image segmentation. In: Navab, N., Hornegger, J., Wells, W.M., Frangi, A.F. (eds.) MICCAI 2015. LNCS, vol. 9351, pp. 234–241. Springer, Cham (2015). https://doi.org/10.1007/978-3-319-24574-4_28

20. Sarkar, P., Etemad, A.: Cardiogan: Attentive generative adversarial network with dual discriminators for synthesis of ECG from PPG. In: Thirty-Fifth AAAI Conference on Artificial Intelligence, AAAI 2021, Thirty-Third Conference on Innovative Applications of Artificial Intelligence, IAAI 2021, The Eleventh Symposium on Educational Advances in Artificial Intelligence, EAAI 2021, Virtual Event, February 2–9, 2021. pp. 488–496. AAAI Press (2021). https://ojs.aaai.org/index.php/AAAI/article/view/16126
21. Wang, L., Zhou, W., Xing, Y., Liu, N., Movahedipour, M., Zhou, X.: A novel method based on convolutional neural networks for deriving standard 12-lead ECG from serial 3-lead ECG. Front. Inf. Technol. Electron. Eng. **20**(3), 405–413 (2019)
22. Zhang, Y.H., Babaeizadeh, S.: Synthesis of standard 12-lead electrocardiograms using two-dimensional generative adversarial networks. J. Electrocardiol. **69**, 6–14 (2021)
23. Zhu, F., Fei, Y., Fu, Y., Liu, Q., Shen, B.: Electrocardiogram generation with a bidirectional LSTM-CNN generative adversarial network. Sci. Rep. **9**, 1–11, 6734 (2019)
24. Zhu, J.Y., Park, T., Isola, P., Efros, A.A.: Unpaired image-to-image translation using cycle-consistent adversarial networks. In: 2017 IEEE International Conference on Computer Vision (ICCV), pp. 2242–2251 (2017). https://doi.org/10.1109/ICCV.2017.244